International Journal of Environmental Sciences
ISSN: 2229-7359
Vol. 11 No. 1s, 2025
https://www.theaspd.com/ijes.php

Representing Thermal Energy in the Atmosphere Based on Data on Sensible Heat, Latent Heat, and Amounts of Thermal Radiation Emitted in Some Iraqi Stations

Ruaa M. Ibrahim[1], Zahraa S. Mahdi[2], Khawla N. Zeki[3], Osama T. Al-Taai[4]*, Zainab M. Abbood[5]
[1,2,3,4,5]Department of Atmospheric Sciences, College of Science, Mustansiriyah University, Baghdad, Iraq
* Corresponding author E-mail: osamaaltaai77@uomustansiriyah.edu.iq

Abstract: *Thermal radiation is the process in which energy, in the form of electromagnetic radiation, is released from a heated surface in all directions and moves at the speed of light straight to its site of absorption. It doesn't need a medium to deliver it. The wavelengths of thermal radiation span from the shortest ultraviolet rays to the longest infrared rays through the visible light spectrum. The temperature of the emitting surface controls the radiant energy's distribution and intensity within this range. According to the Stefan-Boltzmann law, a surface's total radiant heat energy is proportional to the fourth power of its absolute temperature. In addition to surface net solar radiation (SNSR) and surface net solar radiation clear sky (SNSR clear sky) for noon, as well as surface net thermal radiation (SNR) and surface net thermal radiation clear sky (SNTR clear sky) for two times (00;00 am and 12:00 pm), data are collected by latent heat (LH), sensible heat (SH), and satellites recorded by the European Centre for Medium-Range Weather Forecasts Two latitudes (29.55 - 37.225) north of the equator and two longitudes (38.455 - 48.548) east of the Corniche line are covered by the 2021 over Iraq stations selection. The examination of the daily means of LH, SH, SNSR, SNSR clear sky, SNTR, and SNTR clear sky has been our focus otherwise. Spearman's test results demonstrated that, for all stations chosen in Iraq, there is a substantial correlation between thermal radiation types (SNTR clear sky, SNTR, and STRD) and latent heat and sensible heat, and that this correlation is positive for 2021. According to the test findings in Table 1, the Emadiyah station (SH & SNTR) at noon had the highest correlation coefficient in the Spearman's test (0.9), although the correlation coefficient for this station was the lowest across several stations.*

Keywords: *LH, SH, SNSR, SNSR clear sky, SNTR and SNTR clear sky, Iraq.*

INTRODUCTION

When particles in matter move thermally, they emit electromagnetic radiation, which is known as thermal radiation. Thermal radiation travels through matter and vacuum as an electromagnetic wave. The temperature of matter tends to increase when it absorbs thermal radiation [1][2]. Thermal radiation is emitted by any matter that has a temperature higher than absolute zero. A material's electrical, molecular, and lattice oscillations all contribute to the energy output Charge-acceleration or dipole oscillation transform kinetic energy into electromagnetism [3][4][5]. The infrared (IR) spectrum contains the majority of the emission at ambient temperature [6][7]. Together with conduction and convection, thermal radiation is one of the basic processes of heat transmission [8][9]. Thermal radiation is the main way that heat is transferred from the Sun to the Earth. The sky appears to be blue because of the partial absorption and dispersion of this energy in the atmosphere. A large portion of the Sun's energy travels to the surface via the atmosphere, where it is either reflected or absorbed [10] [11] [12]. Things or occurrences that are often invisible to the human eye can be detected via thermal radiation. By detecting infrared light, thermographic cameras provide an image [13] [14]. These pictures can show a scene's temperature gradient and are frequently used to find objects that are hotter than their surroundings [15] [16] [17]. Because of their body temperature, infrared pictures can be utilized to find people or animals in low-light, dark environments [18] [19]. Thermal radiation also includes cosmic microwave background radiation

[20] [21]. Thermal radiation in idealized systems is analyzed using the concept of blackbody radiation [22]. If a radiation object satisfies the physical requirements of a black body in thermodynamic equilibrium, then this model is applicable [23] [24]. Planck's law links the radiative heat flux from a body to its temperature and characterizes the spectrum of blackbody radiation [25]. The radiant intensity is determined by the Stefan–Boltzmann law, while the most likely frequency of the emitted radiation is determined by Wien's displacement law [26]. Quantum electrodynamics (QED) can be used to explain emission and absorption in situations when blackbody radiation is not a reliable approximation [27]. Electromagnetic waves emitted by any matter with a temperature higher than absolute zero are known as thermal radiation. The transformation of thermal energy into electromagnetic energy is reflected in thermal radiation [28]. The kinetic energy of atoms and molecules moving randomly within matter is known as thermal energy. It exists at a temperature that is not zero in all matter. Protons and electrons, which are charged particles, make up these atoms and molecules. Dipole oscillation and charge acceleration are the outcomes of the kinetic interactions between matter particles [29]. This causes linked electric and magnetic fields to be generated electrodynamic ally, which releases photons and radiates energy outside the body. In a vacuum, visible light and other electromagnetic waves will continue to propagate indefinitely [30]. Kirchhoff's law [31] states that the temperature and spectral emissivity of the surface from which thermal radiation is originating are two of the parameters that determine its characteristics. The radiation's characteristic spectrum is a continuous spectrum of photon energies rather than a single frequency, making it non-monochromatic. A black body is defined as one in which the radiating body and its surface are in thermodynamic equilibrium and the surface has complete absorptivity at all wavelengths [32]. Additionally, a black body emits perfectly. Black-body radiation is the radiation produced by such ideal emitters. The emissivity of a body is the ratio of its emission to that of a black body; hence, the emissivity of a black body is 1. All bodies' emissivity, reflectivity, and absorbtivity depend on the radiation's wavelength. Since absorptivity and emissivity are identical at equilibrium for any given wavelength due to reciprocity, a good absorber is inevitably a good emitter, and a poor absorber is a poor emitter [33]. The electromagnetic radiation's wavelength distribution is influenced by temperature [34]. Planck's law describes the power distribution that a black body generates at different frequencies [35]. There is a frequency fmax at which the power released reaches its maximum at any given temperature. The peak frequency fmax is related to the absolute temperature T of the black body, as indicated by Wien's displacement law and the fact that the frequency is inversely proportional to the wavelength [36][37].

With a temperature of about 6000 K, the sun's photosphere mostly produces radiation in the (human-)visible range of the electromagnetic spectrum [38][39]. Light that reaches the surface is either absorbed or reflected by the Earth's atmosphere, which is partially transparent to visible light [40][41]. With a spectral peak at fmax, the absorbed radiation is released from the Earth's surface, simulating the behavior of a black body at 300 K. The atmosphere is mostly opaque at these lower frequencies, absorbing or scattering radiation from the Earth's surface. The majority of this radiation is absorbed and subsequently re-emitted by atmospheric gases, however around 10% of it escapes into space. The planetary greenhouse effect, which contributes to global warming and climate change in general, is caused by the atmosphere's spectral selectivity. It also plays a crucial role in maintaining climate stability when the atmosphere's composition and characteristics remain constant [42].

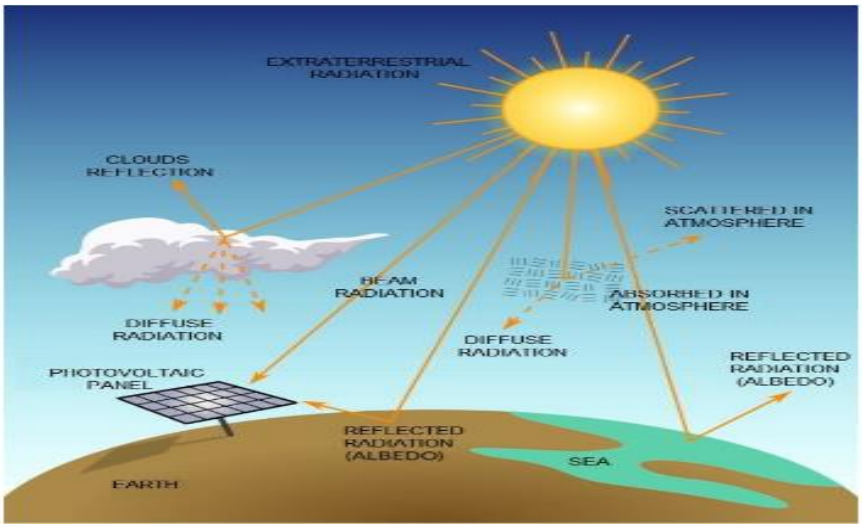

Figure 1. Solar radiation disturbance [43].

Atoms and molecules in matter move randomly, producing thermal radiation. Electromagnetic radiation is produced when charged protons and electrons move [44]. The ability of an object to emit energy as thermal radiation is known as its emissivity. The theoretical extremes of a perfect emitter (blackbody radiator = 1) and a perfect reflector (= 0) are used to quantify the emissivity of heat radiation [45]. Human skin typically has an emissivity of 0.97 or 0.98, which is comparable to the emissivity of ice (0.97), and humans emit large amounts of infrared light [46]. This is because skin contains a lot of water. Thus, variations in skin thermal radiation can be measured clinically using infrared thermal imaging cameras [47].

The origin of solar radiation

In the Sun's interior, hydrogen nuclei fuse and transform into helium through nuclear fusion events [48]. This reaction releases a lot of energy that travels into the sun's interior and stays there for a while, increasing in wavelength until it reaches the sun's surface [49]. We are reached by this light [50]. The thermal energy required for life on Earth is supplied by the sun [51][52]. Because of our distance from the sun, which is approximately 150 million kilometers, the average temperature on Earth is around 14 degrees Celsius, which is a perfect temperature for life [53][54].

Types of solar rays

In Figure 2, the Scientists distinguish three types of rays that make up solar radiation, which include [55]:

1. 1. Infrared rays, also known as thermal rays, are invisible and are thought to make about 50% of all sun radiation. They are crucial to every action and have a wavelength between 0.75 and 4.0 microns (1/1000 of a millimeter). Through the window, sunlight filtered in.
2. 2. The rays of light that are referred to as visible are actually invisible. For instance, the sun's rays, also known as visible light, enter the cosmos without our awareness but light up the transparent material environment where they are scattered, like our atmosphere, or reflected from it, like the moon's surface. The key to lighting the atmosphere is scattering. Knowing that light can be broken down into its constituent elements using a glass prism, daylight is thought to consist of 37% light rays, which have a wavelength between 0.40 and 0.74 microns. During the summer, the intensity of light rays on Earth's surface increases at noon. summertime.

3. Invisible ultraviolet rays, often known as "vital rays," are thought to make up 13% of all solar radiation. Their wavelength ranges from

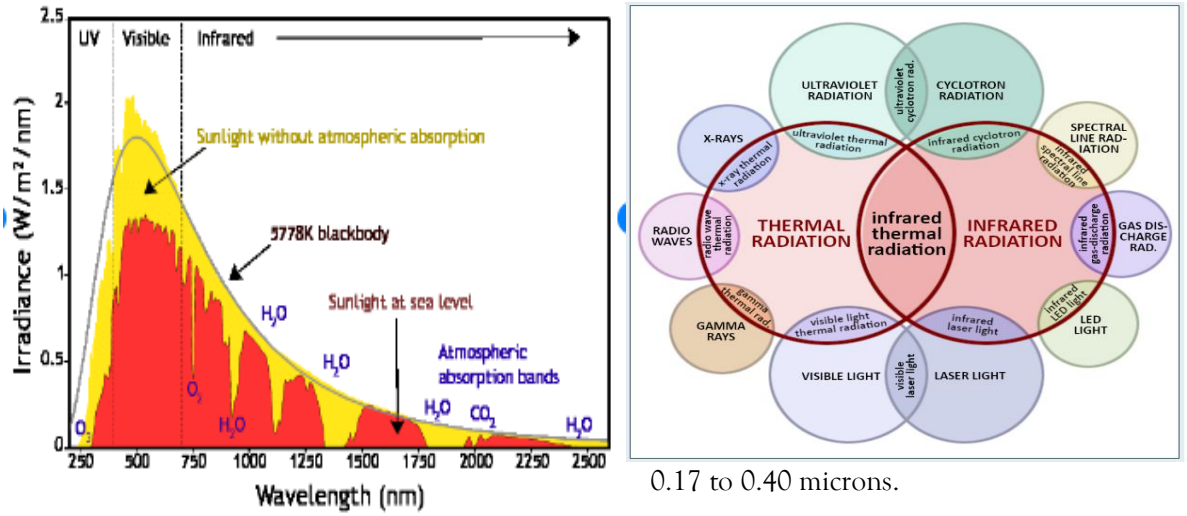

0.17 to 0.40 microns.

Figure 2. Solar and thermal radiation regions [55].

MATERIAL AND METHODS

Study stations and location:

The city of Iraq is the study area. Since 2021 covers two latitudes (29.55°–37.225°) north of the equator and two longitudes (38.455°–48.548°) east of the Corniche line, it is an important year to choose. The daily mean of LH, SH, SNSR, SNSR clear sky, SNTR, and SNTR clear sky for the year 2021 over Iraq were obtained from the European Center for Medium-range Weather Forecasts. as displayed in Figure 3 and Table 1.

Table 1. The meteorological station used in the study [55].

Station	Longitude (degrees)	Latitude (degree)	Elevation (m)
Rutba	40.28	33.03	222
Emadiyah	43.30	37.05	1236
Basrah	47.78	30.52	2
Baghdad	44.4	33.3	32

International Journal of Environmental Sciences
ISSN: 2229-7359
Vol. 11 No. 1s, 2025
https://www.theaspd.com/ijes.php

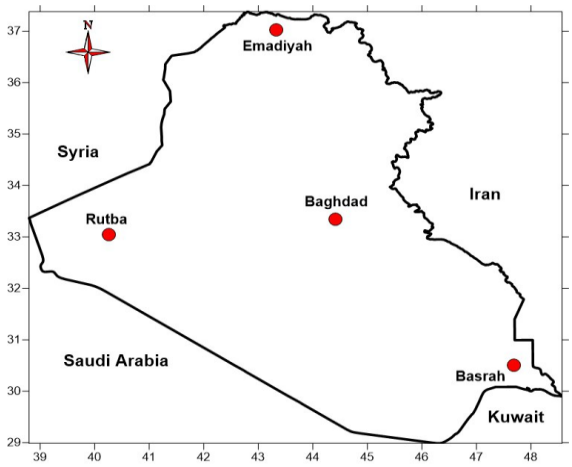

Figure 3. Iraq maps.

Analysis of the behavior of the daily mean of latent and sensible heat over Iraq

Figure 4 shows the daily mean of LH and SH for two times, 00:00 am and 12:00 pm, over Iraq for 2021. The largest amount of LH occurred in Kerbela and a smaller amount in Rutba stations at 00:00 am The largest amount of LH occurred in Emadiyah and a smaller amount in Basrah stations at noon. The largest amount of SH occurred in Hella and a smaller amount in Emadiyah stations at 00:00 am The largest amount of LH occurred in Kerbela and a smaller amount in Emadiyah stations at noon.

This is due to atmospheric and astronomical factors, climatic changes, and the nature of the surface, which contributes to the increase of latent and sensible heat in this region.

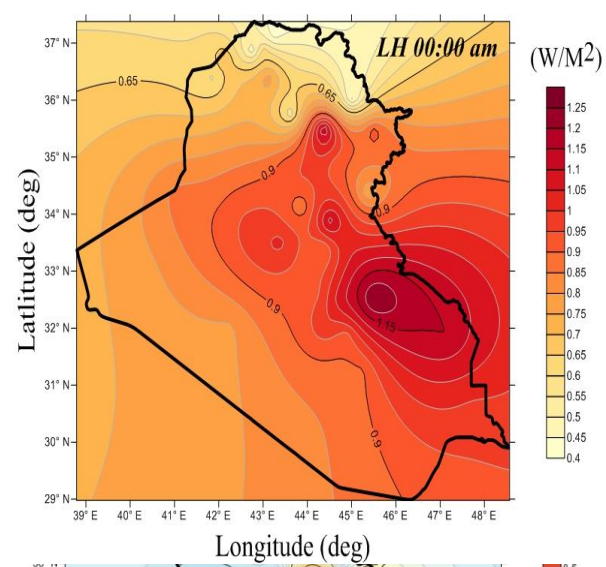

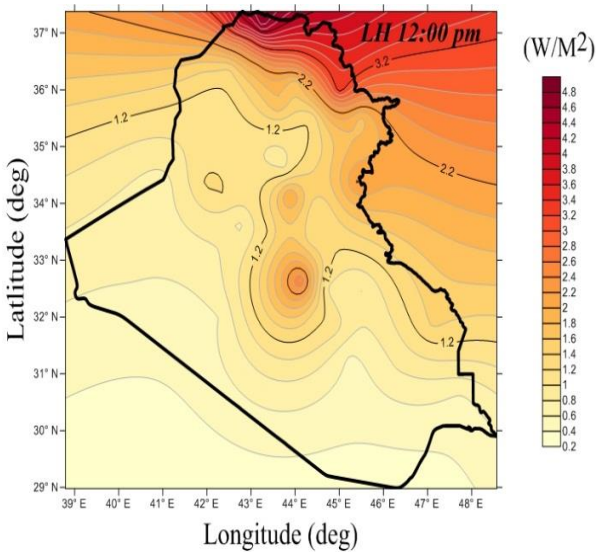

Figure 3. Analysis of the daily mean of latent and sensible heat over Iraq for 2021.

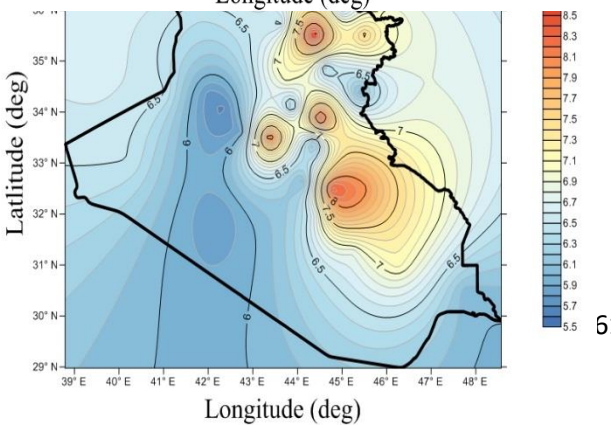

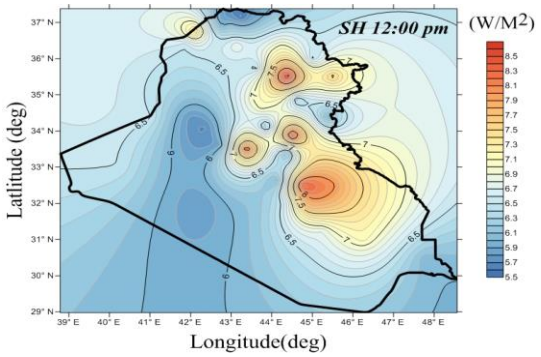

Analysis of the behavior of the daily

mean of thermal heat over Iraq

Figure 4 shows the daily mean of SNTR, SNTR clear sky, and STRD for two times, 00:00 am and 12:00 pm, over Iraq for 2021. The largest amount of SNTR occurred on Ramadi and a smaller amount on Emadiyah stations at 00:00 am The largest amount of SNTR occurred on Samawa and a smaller amount on Emadiyah stations at noon. The largest amount of SNTR clear sky occurred on Nasiriya, and a smaller amount on Emadiyah stations for 00:00 am The largest amount of SNTR clear sky occurred on Nasiriya and a smaller amount on Emadiyah stations for noon. The largest amount of STRD occurred on Amara and a smaller amount on Emadiyah stations for 00:00 am the largest amount of STRD occurred on Amara and a smaller amount on Emadiyah stations for noon. This is because thermal radiation is present during the day and night when it is emitted as a result of the absorption of solar radiation by the Earth's surface, or as a result of the components of the atmosphere, which represent clouds, gases, and aerosols, absorbing solar radiation and then emitting thermal radiation during the day and night.

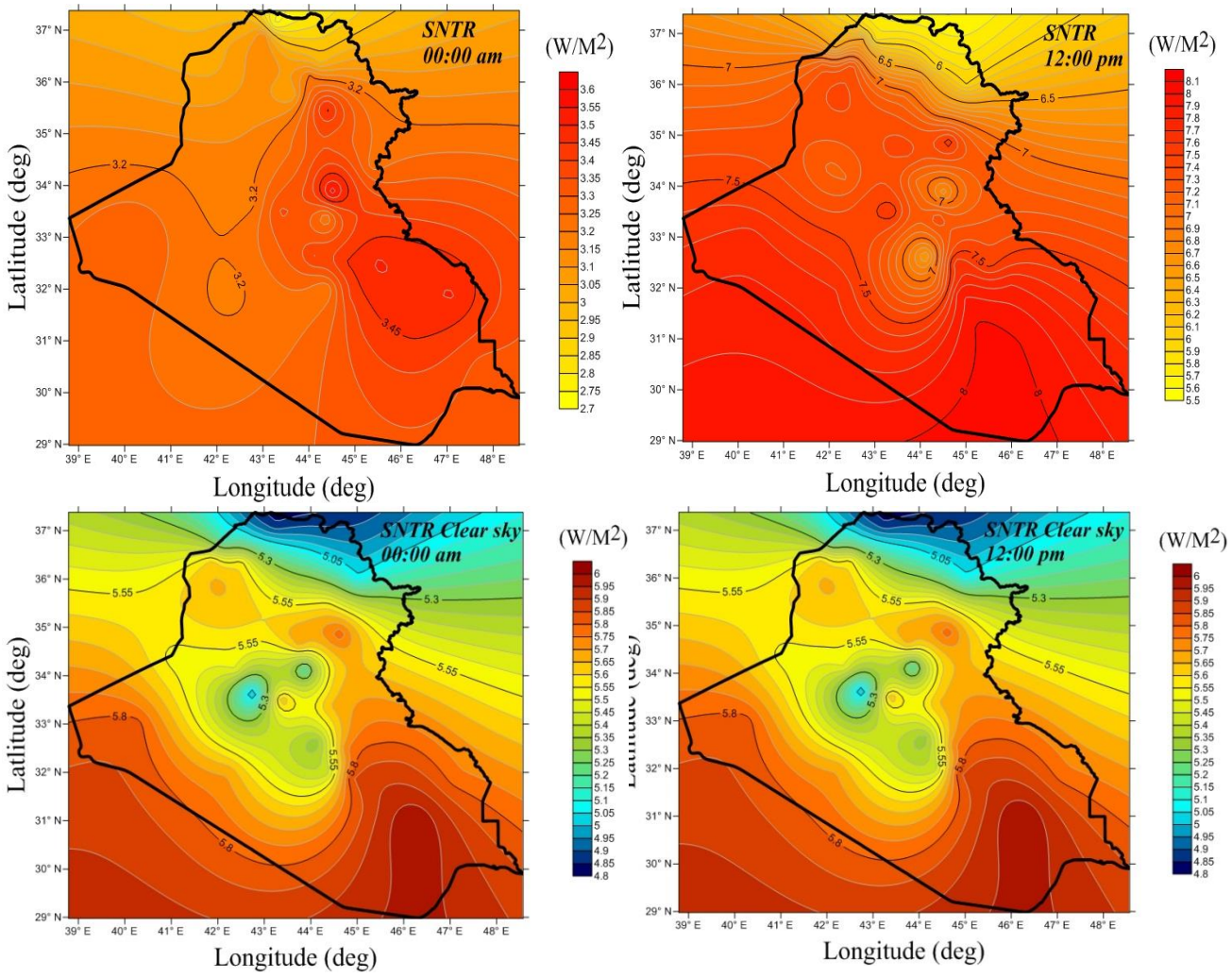

International Journal of Environmental Sciences
ISSN: 2229-7359
Vol. 11 No. 1s, 2025
https://www.theaspd.com/ijes.php

Figure 4. Analysis of the daily mean of latent and sensible heat over Iraq for the year 2021.

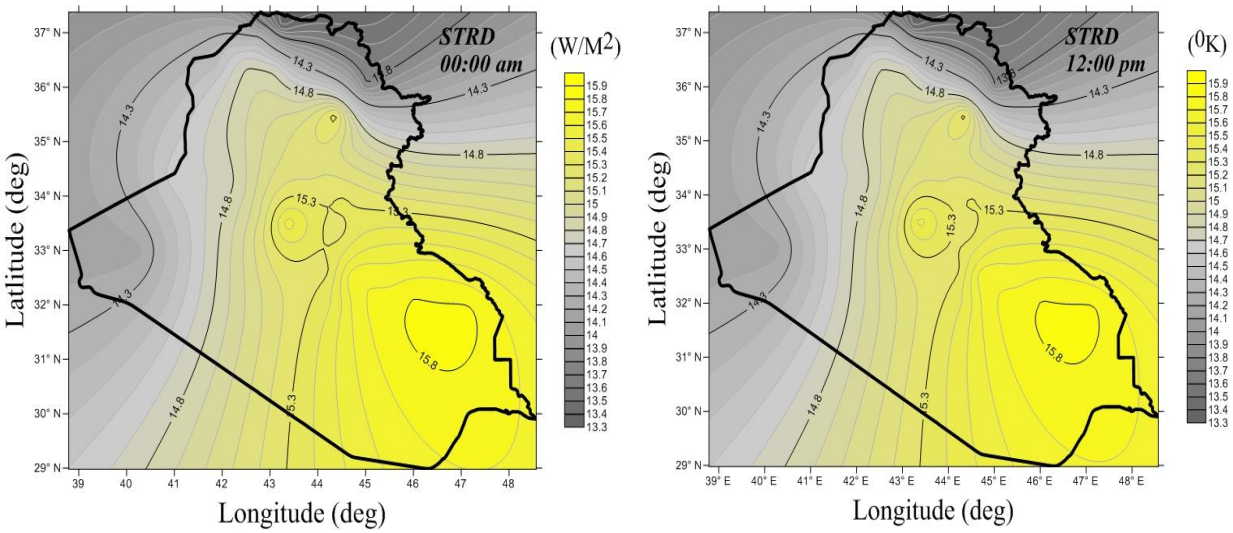

Followed Figure 4.

Analysis of the behavior of the daily mean of solar radiation over Iraq

Figure 5 shows the daily mean of SNSR, SNSR clear sky, and TOA ISR for noon over Iraq for 2021. The largest amount of SNSR occurred on Kerbela and a smaller amount on Basrah stations for 12:00 pm The largest amount of SNSR in clear sky occurred on Dukcan and a smaller amount on Anah stations for noon. The largest amount of TOA ISR occurred on Rutba and a smaller amount on Dukcan stations at noon. This is because solar radiation is present during the day when it travels through the atmosphere and is subjected to scattering, absorption, and reflection due to the components of the atmosphere, which are clouds and gases. A large portion of aerosols and solar radiation is reflected off the Earth's surface.

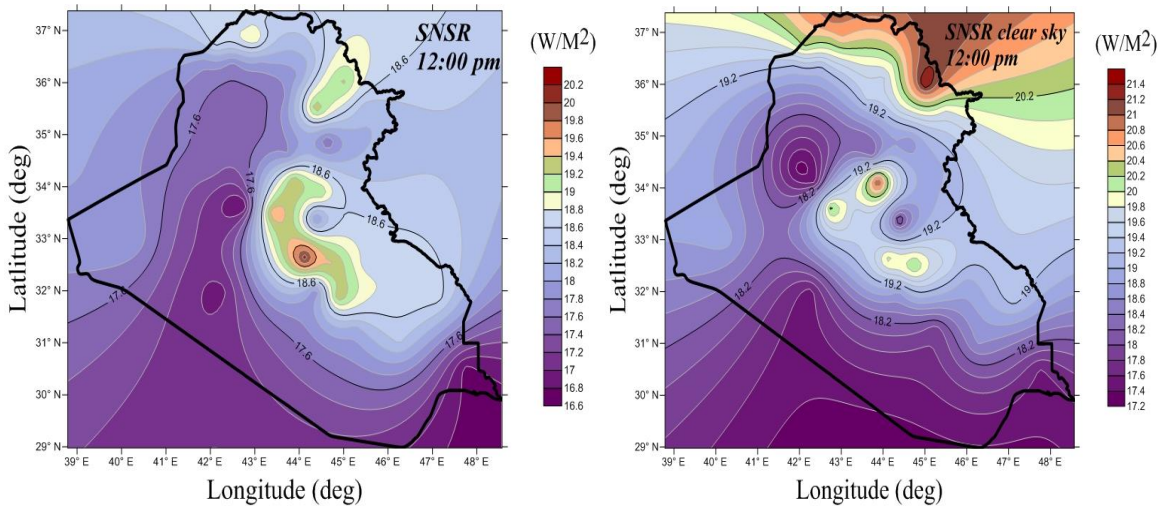

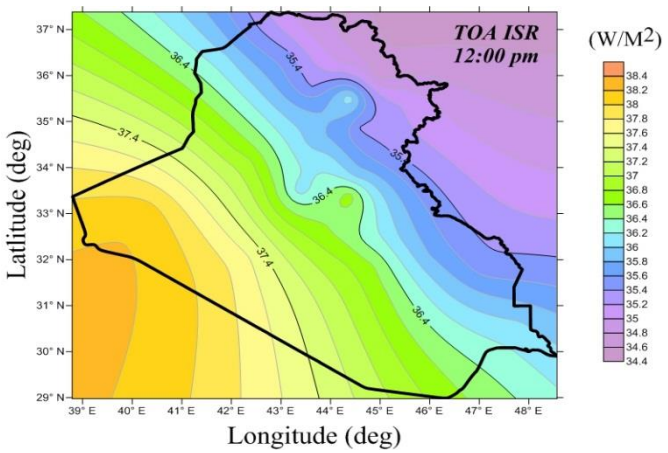

Figure 5. Analysis of the daily mean of solar heat over Iraq for the year 2021.

Analysis of the behavior of the daily mean temperature over Iraq

Figure 6 displays the average daily temperature over Iraq in 2021 at two different hours, 0:00 am and 12:00 pm. At midday, the highest temperature was recorded in Basrah and the lowest in Emadiyah stations, while the highest temperature was recorded in Nasiriya and the lowest in Emadiyah stations. This is due to the temperature being higher during the day than at night, and the southern regions are hotter than the northern regions. This is due to solar radiation, the angle of incidence of radiation, and the nature of the region.

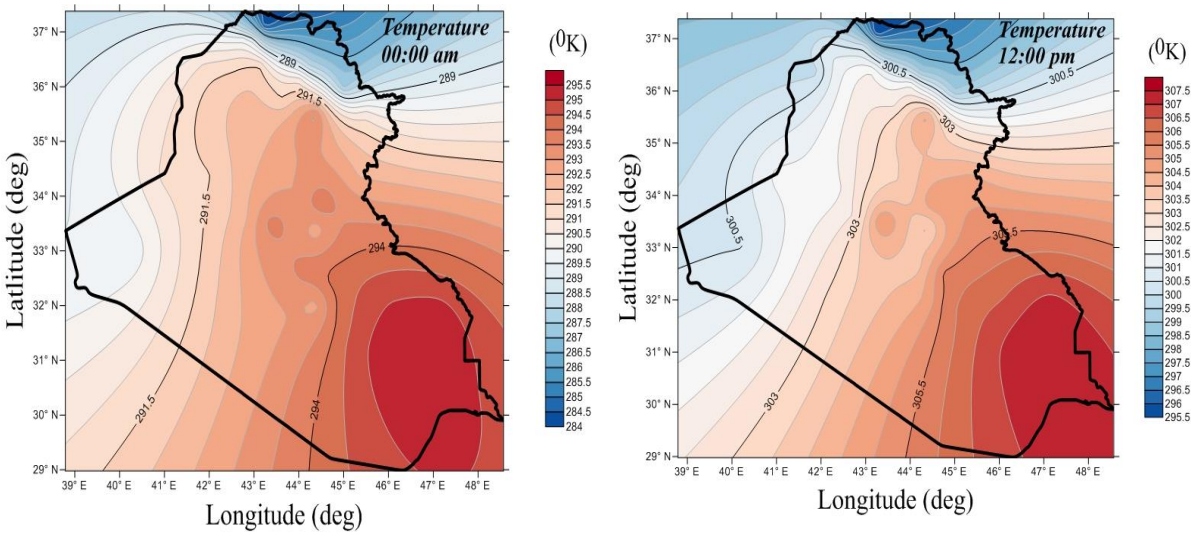

Figure 6. Analysis of the daily mean of temperature over Iraq for 2021.

The Relationship Between thermal radiation types with (latent heat and sensible heat)

In Figures 7 and 8, For all stations chosen in Iraq, the Spearman's test results demonstrated a substantial association between thermal radiation types (SNTR clear sky, SNTR, and STRD) and latent heat and sensible heat, with a positive relationship for 2021. According to the test results in Table 1, the Emadiyah station (SH and SNTR) at noon had the highest correlation coefficient in the Spearman's test (0.9), although the correlation coefficient for this station was the lowest across

numerous stations. It was determined that there is a weak but inverse relationship between thermal radiation and sensible heat and latent heat. Latent and sensible heat will increase through atmospheric components including clouds, gases, and aerosols when thermal radiation in the atmosphere rises.

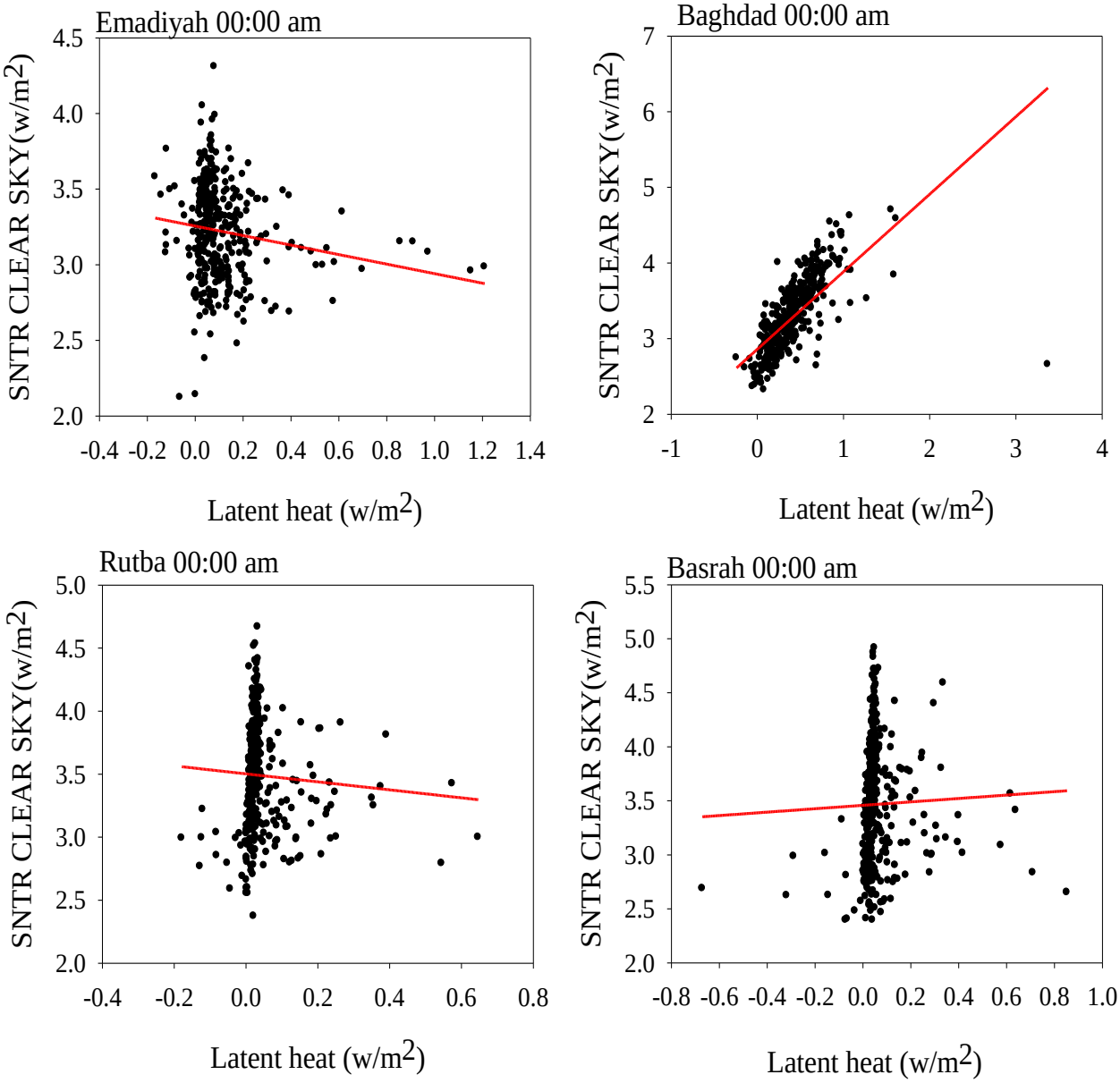

International Journal of Environmental Sciences
ISSN: 2229-7359
Vol. 11 No. 1s, 2025
https://www.theaspd.com/ijes.php

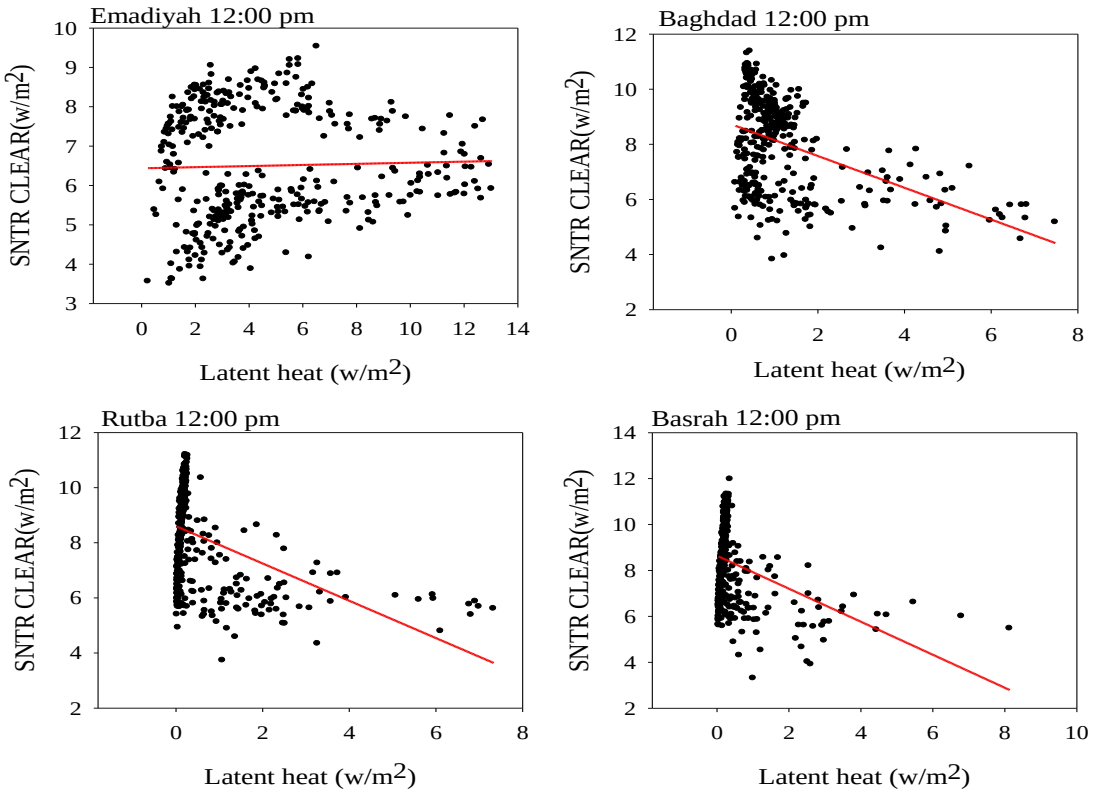

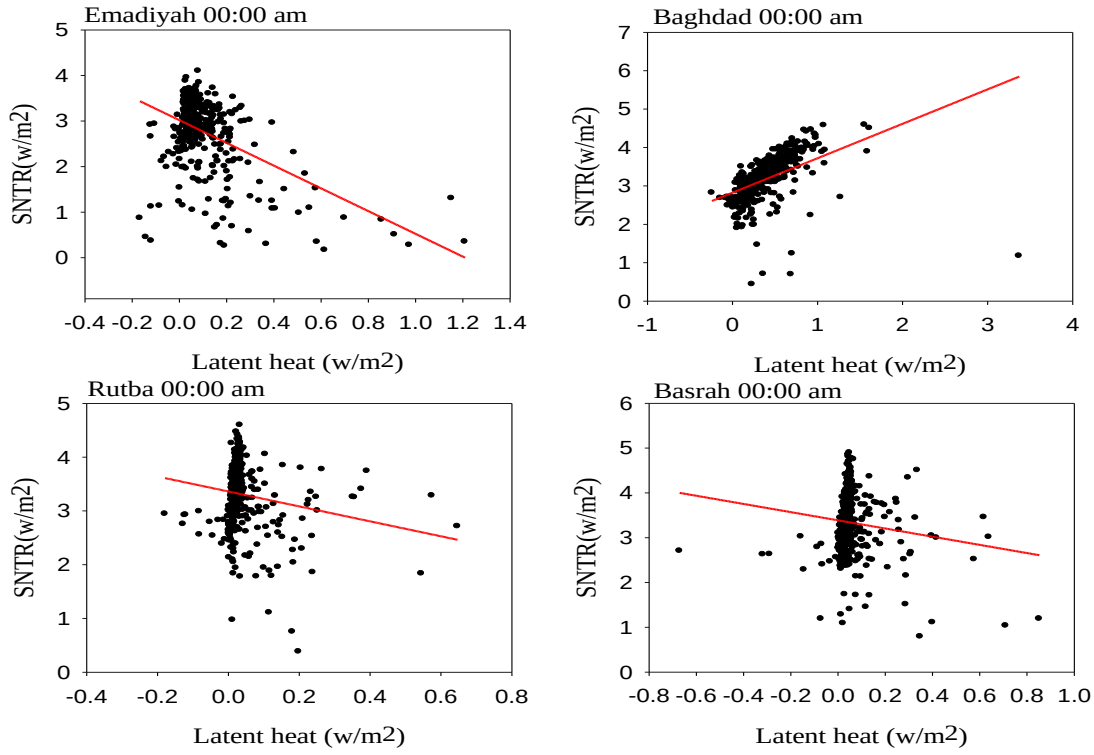

International Journal of Environmental Sciences
ISSN: 2229-7359
Vol. 11 No. 1s, 2025
https://www.theaspd.com/ijes.php

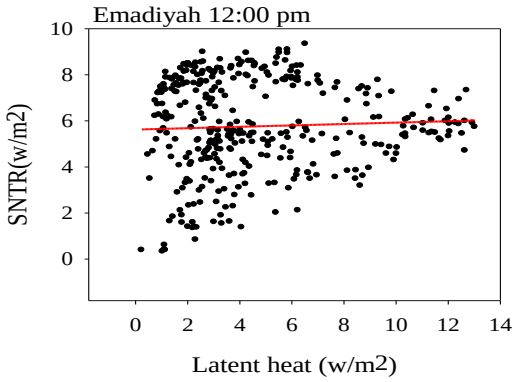

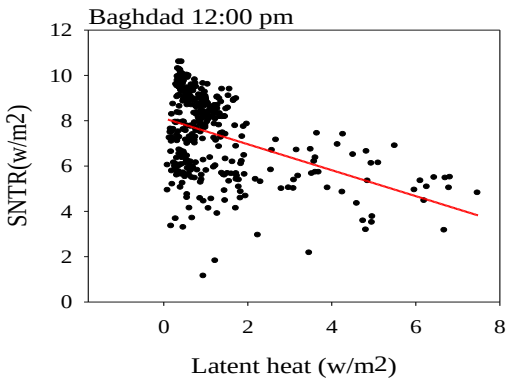

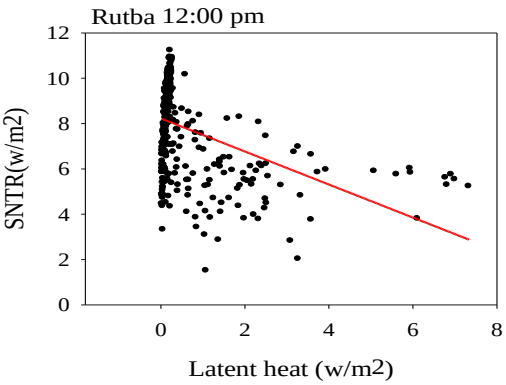

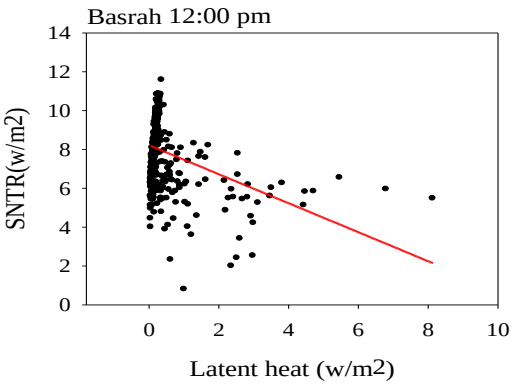

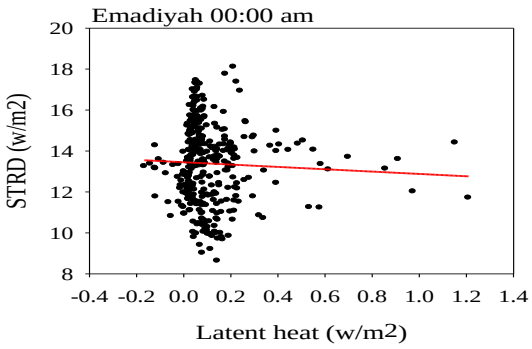

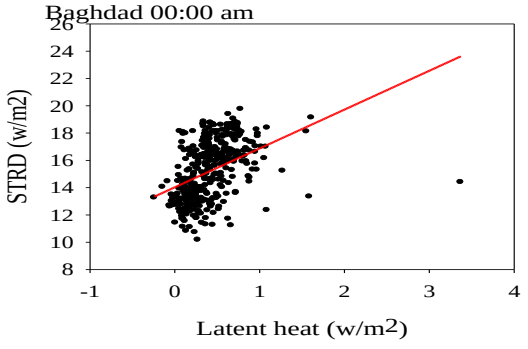

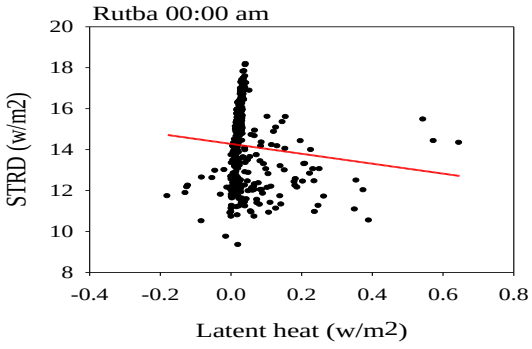

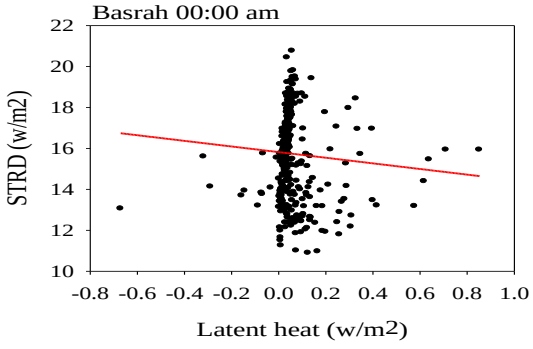

International Journal of Environmental Sciences
ISSN: 2229-7359
Vol. 11 No. 1s, 2025
https://www.theaspd.com/ijes.php

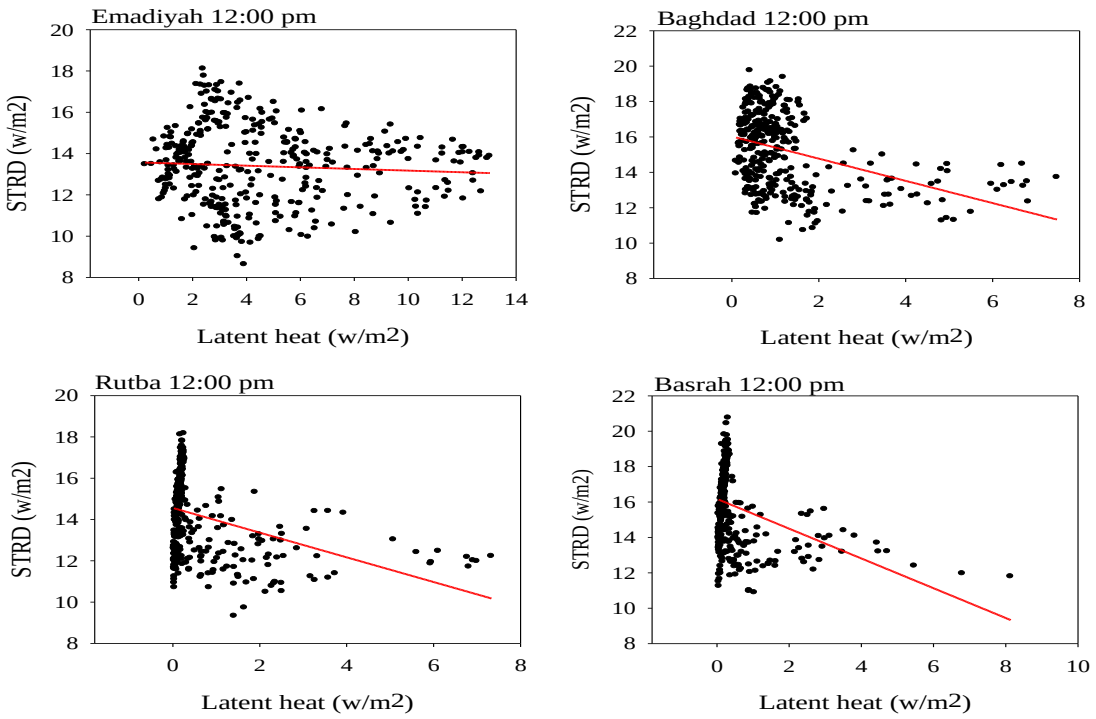

Figure 7. The relationship between the daily mean of latent heat and (SNTR clear sky, SNTR, and STRD) of Iraqi Stations: (a) Emadiyah, (b) Baghdad, (c) Rutba, and (d) Basra for two times, 00:00 am and 12:00 pm.

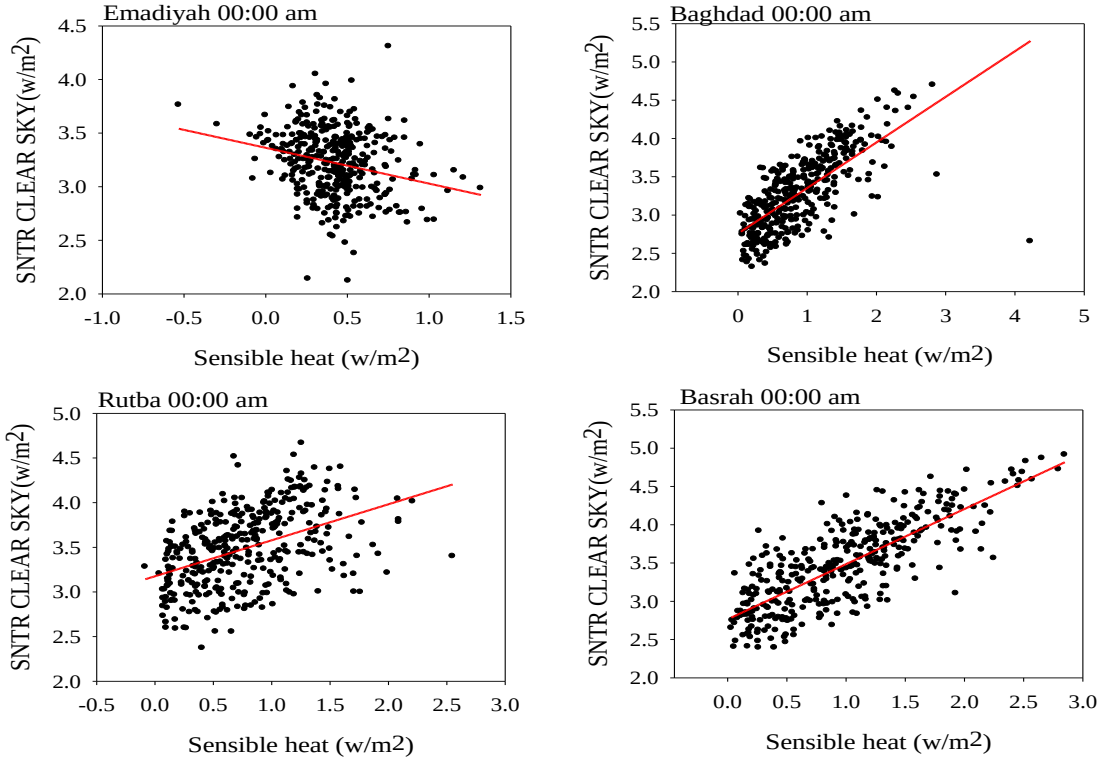

International Journal of Environmental Sciences
ISSN: 2229-7359
Vol. 11 No. 1s, 2025
https://www.theaspd.com/ijes.php

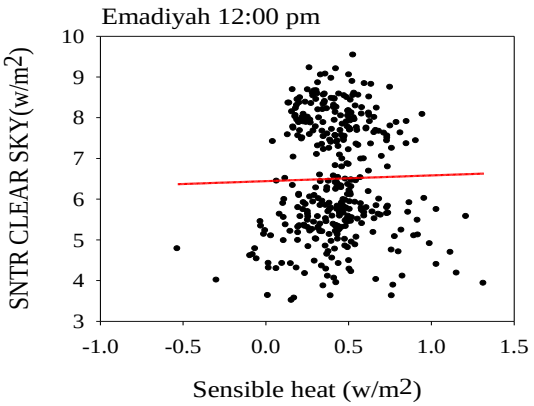

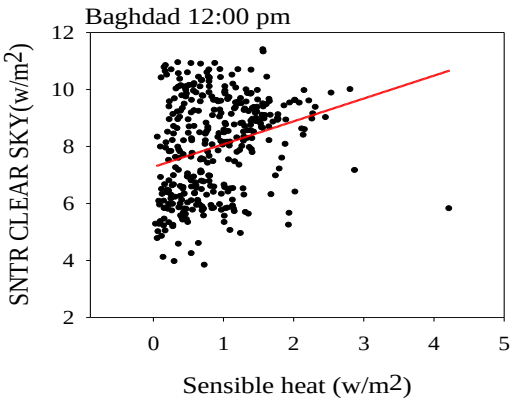

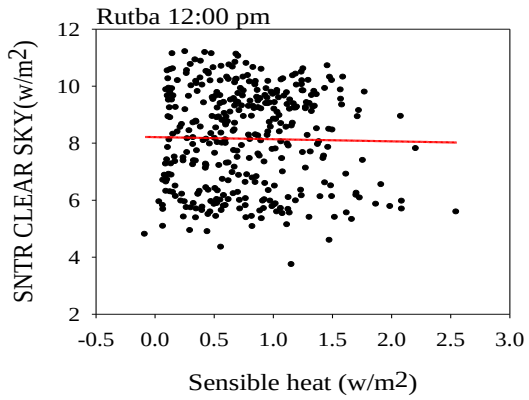

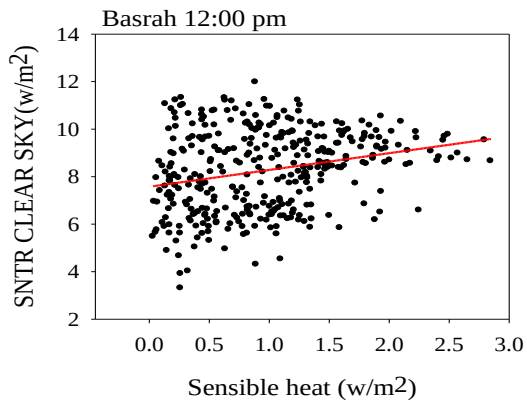

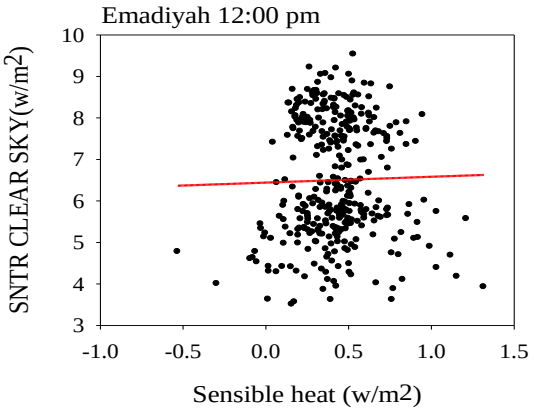

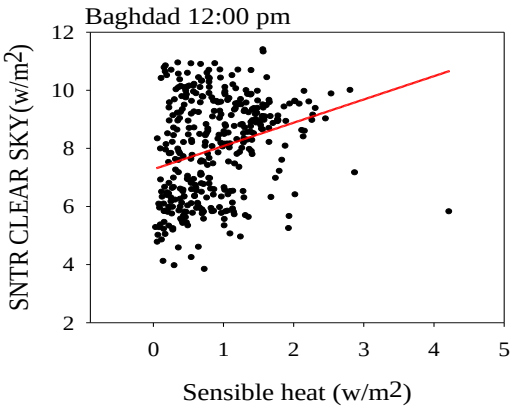

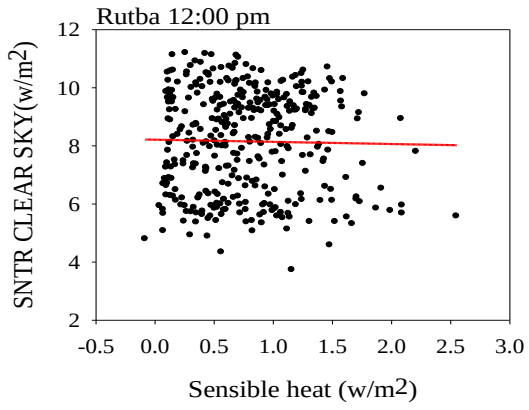

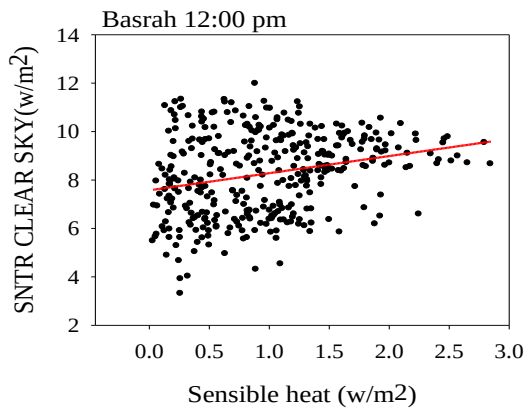

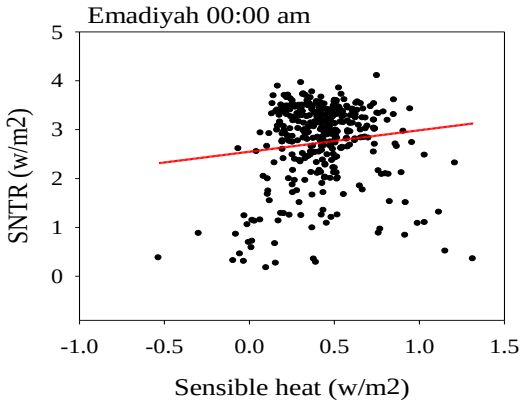
Emadiyah 00:00 am
SNTR (w/m2)
Sensible heat (w/m2)

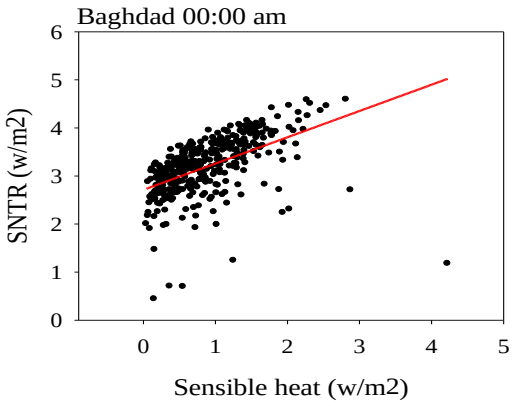
Baghdad 00:00 am
SNTR (w/m2)
Sensible heat (w/m2)

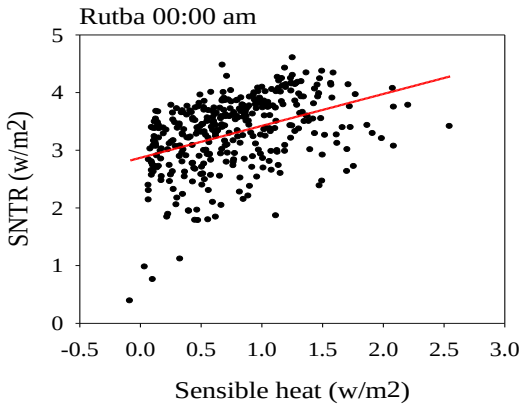
Rutba 00:00 am
SNTR (w/m2)
Sensible heat (w/m2)

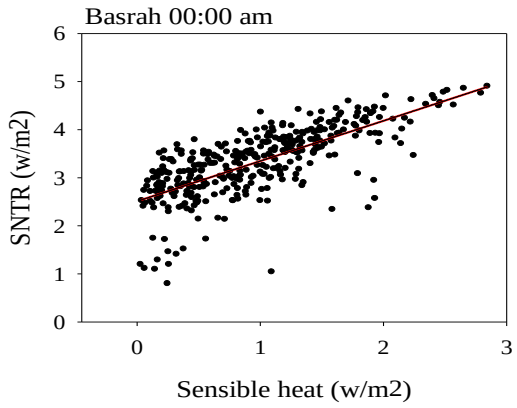
Basrah 00:00 am
SNTR (w/m2)
Sensible heat (w/m2)

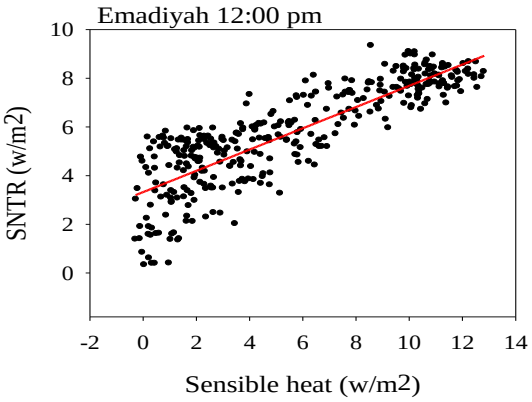
Emadiyah 12:00 pm
SNTR (w/m2)
Sensible heat (w/m2)

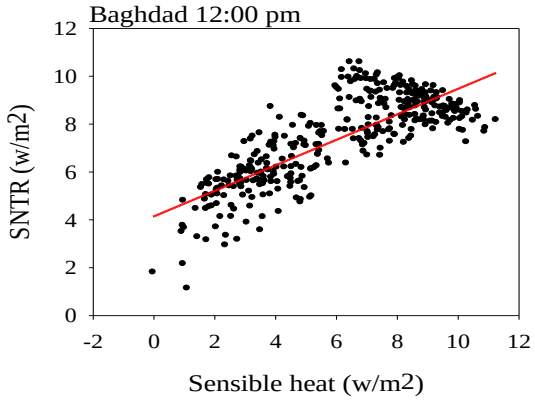
Baghdad 12:00 pm
SNTR (w/m2)
Sensible heat (w/m2)

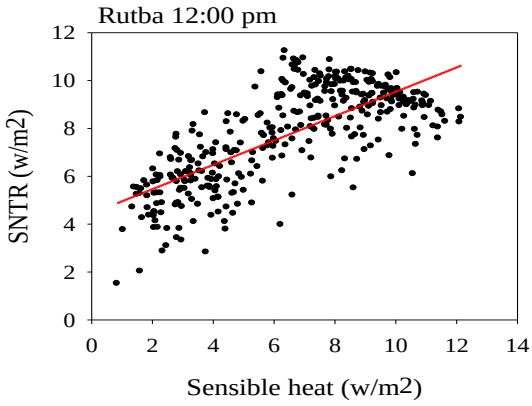
Rutba 12:00 pm
SNTR (w/m2)
Sensible heat (w/m2)

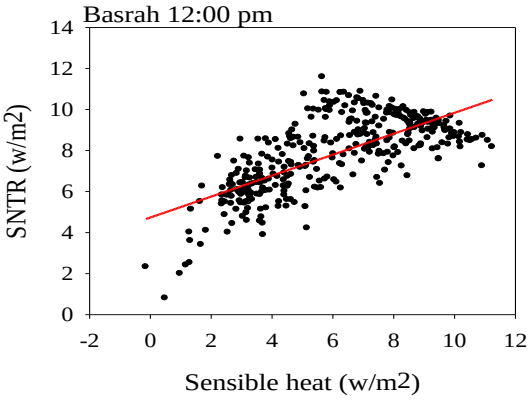
Basrah 12:00 pm
SNTR (w/m2)
Sensible heat (w/m2)

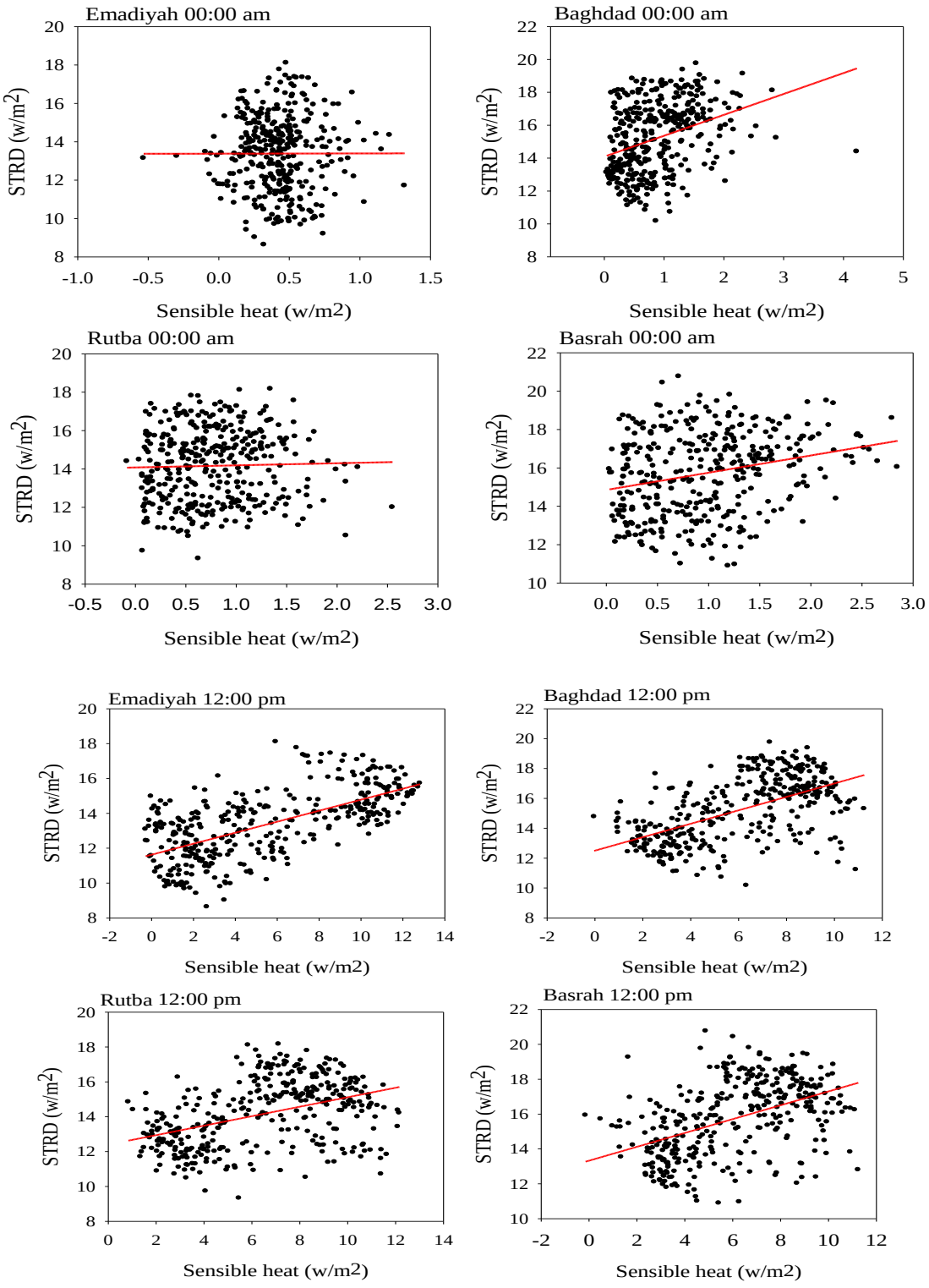

Figure 8. The relationship between the daily mean of sensible heat and (SNTR clear sky, SNTR, and STRD) of Iraqi Stations: (a) Emadiyah, (b) Baghdad, (c) Rutba, and (d) Basra for two times, 00:00 am and 12:00 pm.

Table 2: The relationship between LH and SH with the types of thermal radiation at the time (00:00 am and 12:00 pm) for the year 2021 over the Iraqi stations.

Hour	**Spearman rho**		**Linear regression Simple**	
At the time 00:00 am	**(LH and SNTR CLEAR)**	**Correlation degree**	**P-value**	**Interpretation of the relationship**
Emadiyah	0.2	Low inverse correlation	0.0026	Linear relation
Baghdad	0.7	High positive correlation	0.2621	Linear relation
Rutba	0.06	Very low inverse correlation	0.2621	Non-Linear relation
Basrah	0.03	Very Low positive correlation	0.5440	Non-Linear relation
At the time 12:00 pm	**(LH and SNTR CLEAR)**	**Correlation degree**	**P-value**	**Interpretation of the relationship**
Emadiyah	0.03	Very Low inverse correlation	0.5592	Non-Linear relation
Baghdad	0.5	Medium inverse correlation	0.001	Linear relation
Rutba	0.5	Medium inverse correlation	0.001	Linear relation
Basrah	0.4	Medium inverse correlation	0.001	Linear relation
At the time 00:00 am	**(LH and SNTR)**	**Correlation degree**	**P-value**	**Interpretation of the relationship**
Emadiyah	-0.5	Medium inverse correlation	0.001	Linear relation
Baghdad	0.5	Medium positive correlation	0.001	Linear relation
Rutba	-0.2	Low inverse correlation	0.0007	Linear relation
Basrah	-0.2	Low inverse correlation	0.0057	Linear relation
At the time 12:00 pm	**(LH and SNTR)**	**Correlation degree**	**P-value**	**Interpretation of the relationship**
Emadiyah	- 0.04	Very Low inverse correlation	0.3730	Non-Linear relation
Baghdad	-0.4	Medium inverse correlation	0.001	Linear relation
Rutba	-0.5	Medium inverse correlation	0.001	Linear relation

Basrah	-0.4	Medium inverse correlation	0.001	Linear relation
At the time 00:00 am	**(LH and STRD)**	**Correlation degree**	**P-value**	**Interpretation of the relationship**
Emadiyah	-0.05	Very Low inverse correlation	0.3792	Non-Linear relation
Baghdad	0.42	Medium positive correlation	0.001	Linear relation
Rutba	-0.10	Very low inverse correlation	0.0483	Linear relation
Basrah	-0.07	Very Low inverse correlation	0.169	Non-Linear relation
At the time 12:00 pm	**(LH and STRD)**	**Correlation degree**	**P-value**	**Interpretation of the relationship**
Emadiyah	-0.064	Very Low inverse correlation	0.21	Non-Linear relation
Baghdad	-0.39	Medium inverse correlation	0.001	Linear relation
Rutba	-0.22	Low inverse correlation	0.001	Linear relation
Basrah	-0.39	Medium inverse correlation	0.37	Linear relation
At the time 00:00 am	**(SH and SNTR CLEAR)**	**Correlation degree**	**P-value**	**Interpretation of the relationship**
Emadiyah	-0.25	Low positive correlation	0.001	Linear relation
Baghdad	0.72	Medium positive correlation	0.001	Linear relation
Rutba	0.44	Low positive correlation	0.001	Linear relation
Basrah	0.80	Low positive correlation	0.001	Linear relation
At the time 12:00 pm	**(SH and SNTR CLEAR)**	**Correlation degree**	**P-value**	**Interpretation of the relationship**
Emadiyah	-0.02	Very low positive correlation	0.6690	Non-Linear relation
Baghdad	0.27	Low positive correlation	0.001	Linear relation
Rutba	-0.02	Very Low positive correlation	0.7020	Linear relation
Basrah	0.25	Low positive correlation	0.001	Linear relation
At the time 00:00 am	**(SH and SNTR)**	**Correlation degree**	**P-value**	**Interpretation of the relationship**

Emadiyah	0.12	Low positive correlation	0.001	Linear relation
Baghdad	0.53	Medium positive correlation	0.001	Linear relation
Rutba	0.41	Medium positive correlation	0.001	Linear relation
Basrah	0.72	High positive correlation	0.001	Linear relation
At the time 12:00 pm	**(SH and SNTR)**	**Correlation degree**	**P-value**	**Interpretation of the relationship**
Emadiyah	0.9	Very High positive correlation	0.001	Linear relation
Baghdad	0.80	High positive correlation	0.001	Linear relation
Rutba	0.73	High positive correlation	0.001	Linear relation
Basrah	0.71	High positive correlation	0.001	Linear relation
At the time 00:00 am	**(SH and STRD)**	**Correlation degree**	**P-value**	**Interpretation of the relationship**
Emadiyah	0.0014	Very positive correlation	0.9794	Non-Linear relation
Baghdad	0.4	Medium positive correlation	0.001	Linear relation
Rutba	0.0276	Very low positive correlation	0.5993	Non-Linear relation
Basrah	0.2577	Low positive correlation	0.001	Linear relation
At the time 00:00 am	**(SH and STRD)**	**Correlation degree**	**P-value**	**Interpretation of the relationship**
Emadiyah	0.7	High positive correlation	0.001	Linear relation
Baghdad	0.6	Medium positive correlation	0.001	Linear relation
Rutba	0.41	Medium positive correlation	0.001	Linear relation
Basrah	0.50	Medium positive correlation	0.001	Linear relation

CONCLUSIONS

- The largest amount of LH occurred in Kerbela and a smaller amount on Rutba stations at 00:00 am The largest amount of LH occurred in Emadiyah and a smaller amount on Basrah stations at noon. The largest amount of SH occurred in Hella and a smaller amount in Emadiyah stations at 00:00 am, the largest amount of LH occurred in Kerbela and a smaller amount in Emadiyah stations at noon.
- The largest amount of SNTR occurred on Ramadi and a smaller amount on Emadiyah stations at 00:00 am The largest amount of SNTR occurred on Samawa and a smaller amount on Emadiyah stations at noon. The largest amount of SNTR clear sky occurred in Nasiriya, and a smaller amount in Emadiyah stations at 00:00 am, and the largest amount

of SNTR clear sky occurred in Nasiriya and a smaller amount in Emadiyah stations at noon. The largest amount of STRD occurred on Amara and a smaller amount in Emadiyah stations at 00:00 am, the largest amount of STRD occurred on Amara and a smaller amount in Emadiyah stations at noon.

- The largest amount of temperature occurred in Nasiriya and the least amount in Emadiyah stations, while at noon, the largest amount of temperature occurred in Basrah and a smaller amount in Emadiyah stations.
- For all stations chosen in Iraq, the Spearman's test results demonstrated a substantial association between thermal radiation types (SNTR clear sky, SNTR, and STRD) and latent heat and sensible heat, with a positive relationship for 2021. According to the test findings in Table 1, the Emadiyah station (SH, SNTR) at midday had the highest correlation coefficient in the Spearman's test (0.9), whereas numerous other stations had the lowest correlation coefficient value.

ACKNOWLEDGMENT

Both Mustansiriyah University and the European Centre for Medium-Range Weather Forecasts (ECMWF) are acknowledged.

REFERENCES

1. Ahmad, M.J. and G. Tiwari, Solar radiation models—A review. International Journal of Energy Research, 2011. 35(4): p. 271-290.
2. Abd, N.M., Abbood, Z.M., Mohammed, N.A., Al-Taai, O.T., Nassif, W.G., Impact of Acid Gases on Total Precipitation Over Iraqi Stations. Nature Environment and Pollution Technology, 2025, 24, pp. 439–448.
3. Sengupta, M., et al., The national solar radiation database (NSRDB). Renewable and sustainable energy reviews, 2018. 89: p. 51-60.
4. Nassif, W.G., O.T. Al-Taai, and Z.M. Abbood. The influence of solar radiation on ozone column weight over Baghdad city, in IOP Conference Series: Materials Science and Engineering. 2020. IOP Publishing.
5. Iqbal, M., An introduction to solar radiation. 2012: Elsevier.
6. Zhang, J., et al., A critical review of the models used to estimate solar radiation. Renewable and Sustainable Energy Reviews, 2017. 70: p. 314-329.
7. Musacchio, C., G. Coppa, and A. Merlone, An experimental method for evaluation of the snow albedo effect on near-surface air temperature measurements. Meteorological Applications, 2019. 26(1): p. 161-170.
8. Abbood, Z.M. and O.T. Al-Taai, Data analysis for cloud cover and rainfall over Baghdad city, Iraq. Plant Archives, 2020. 20(1): p. 822-826.
9. Katiyar, A. and C. Pandey, A review of solar radiation models—Part I. Journal of Renewable Energy, 2013. 2013(1): p. 168048.
10. Abbood, Z.M. and O.T. Al-Taai, Calculation of absorption and emission of thermal radiation by clouds cover. ARPN Journal of Engineering and Applied Sciences, 2018. 13(24): p. 9446-9456.
11. Hassan, A.S., Kadhum, J.H., Alsalhy, S.N., Al-Taai, O.T., Nanosensor-based satellite images and GIS filter for urban expansion analysis and its impact on climate change. Experimental and Theoretical Nanotechnology, 2025, 2025(Special Issue), pp. 335–346.

12. Al-Taai, O.T., Z.M. Abbood, and J.H. Kadhum, Determination Stability Potential Energy of Thunderstorms for Some Severe Weather Forecasting Cases in Baghdad City. Journal of Green Engineering (JGE), 2021. 11(1): p. 779-794.
13. Mahdi, Z.S., Z.M. Abbood, and O.T. Al-Taai, Thunderstorm dynamic analysis based on total precipitation over Iraq. J. Eng. Sci. Technol, 2021. 16: p. 62-70.
14. Abbood, Z.M., O.T. Al-Taai, and W.G. Nassif, Impact of wind speed and direction on low cloud cover over Baghdad city. Current Applied Science and Technology, 2021: p. 590-600.
15. Abbood, Z.M., M.H. Al-Jiboori, and O.T. Al-Taai. Temporal and Spatial Analysis of Particulate Matter Concentrations in Iraq. In IOP Conference Series: Earth and Environmental Science. 2023. IOP Publishing.
16. Al-Taai, O.T. and Z.M. Abbood, Analysis of the convective available potential energy by precipitation over Iraq using ECMWF data for the period of 1989–2018. Scientific Review Engineering and Environmental Sciences, 2020. 29(2): p. 196-211.
17. Al-Taai, O.T. and Z.M. Abbood, Analysis of convective available potential energy by convective and total precipitation over Iraq. Indian J. Ecology, 2020. 47: p. 263-269.
18. Badescu, V., Modeling solar radiation at the Earth's surface. Springer Verlag, Berlin/Heidelberg, 2008.
19. W. G. Nassif, O. T. Al-Taai, and Z. M. Abbood, "The Influence of Solar Radiation on Ozone Column Weight Over Baghdad City," IOP Conference Series: Materials Science and Engineering, IOP Publishing, vol. 928, no. 7, p. 072089, 2020.
20. Z. M. Abbood, and O. T. Al-Taai, "Data Analysis for Cloud Cover and Rainfall over Baghdad City, Iraq," Plant Archives, vol. 20, no. 1, pp. 822-826, 2020.
21. Z. M. Abbood, and O. T. Al-Taai, "Calculation of Absorption and Emission of Thermal Radiation by Clouds Cover," ARPN Journal of Engineering and Applied Sciences, vol. 13, no. 24, pp. 9446-9456, 2018.
22. S. A. Hashim, W. G. Nassif, B. I. Wahab, Z. M. Abbood, O. T. Al-Taai, and Z. S. Mahdi, "Impact of COVID-19 on Aerosol Optical Depth and Particulate Matter over Iraq," Journal of Engineering Science and Technology, vol. 17, pp. 12-20, 2022.
23. O. T. Al-Taai, Z. M. Abbood, and J. H. Kadhum, "Determination Stability Potential Energy of Thunderstorms for Some Severe Weather Forecasting Cases in Baghdad City," Journal of Green Engineering, vol. 11, no. 1, pp. 779-794, 2021.
24. S. A. Hashim, J. H. Kadhum, Z. M. Abbood, O. T. Al-Taai, and W. G. Nassif, "Determination of the Dynamics of Thunderstorms Through the Dry Adiabatic Lapse Rate and Environmental Lapse Rate," Nature Environment and Pollution Technology, vol. 22, no. 3, pp. 1447-1455, 2023.
25. W. G. Nassif, F. H. Lagenean, and O. T. Al-Taai, "Impact of Vegetation Cover on Climate Change in Different Regions of Iraq," Caspian Journal of Environmental Sciences, vol. 21, no. 2, pp. 333-342, 2023.
26. R. S. Al-Awadi, O. T. Al-Taai, and S. A. Abdullah, "Assessment of Outer Space Events on Troposphere and Climate Change over Iraq," Iraqi Journal of Science, vol. 64, no. 8, pp. 4278-4289, 2023.
27. G. A. Redah, M. H. Al-Jiboori, and O. T. Al-Taai, "Turbulent Diffusion Effect on PM2.5 Concentration Above an Urban Canopy," IOP Conference Series: Earth and Environmental Science, IOP Publishing, vol. 1223, no. 1, p. 012005, 2023.
28. Z. M. Abbood, M. H. Al-Jiboori, and O. T. Al-Taai, "Temporal and Spatial Analysis of Particulate Matter Concentrations in Iraq," IOP Conference Series: Earth and Environmental Science, IOP Publishing, vol. 1215, no. 1, p. 012018, 2023.

29. O. T. Al-Taai, S. A. Hashim, W. G. Nassif, and Z. M. Abbood, "Interference between Total Solar Radiation and Cloud Cover over Baghdad City," Journal of Physics: Conference Series, vol. 2114, no. 1, p. 012070, 2021.
30. A. Al-Behadili, A. H. A. Al-Muhyi, and O. T. Al-Taai, "Analyzing the Oil Pollution Resulting from The Iraqi Oil Ports in The Northern Arabian Gulf Using the GNOME Model," AIP Conference Proceedings, AIP Publishing, vol. 2830, no. 1, p. 050004, 2023.
31. G. A. Redah, M. H. Al-Jiboori, and O. T. Al-Taai, "A Study of Turbulent Fluctuation of Three-Component Wind and Air Temperature in the Surface Layer of Baghdad Urban," IOP Conference Series: Earth and Environmental Science, IOP Publishing, vol. 1223, no. 1, p. 012005, 2023.
32. Z. M. Abbood, O. T. Al-Taai, and W. G. Nassif, "Impact of Wind Speed and Direction on Low Cloud Cover over Baghdad City," Current Applied Science and Technology, vol. 21, no. 3, pp. 590-600, 2021.
33. T. K. Jawad, O. T. Al-Taai, and Y. K. Al-Timimi, "Evaluation of drought in Iraq using DSI by remote sensing," Iraqi Journal of Agricultural Sciences, vol. 49, no. 6, pp. 1132-1145, 2018.
34. O. T. Al-Taai, "Preface," IOP Conference Series: Earth and Environmental Science, vol. 1223, no. 1, p. 011001, 2023.
35. W. G. Nassif, I. K. Al-Ataby, O. T. Al-Taai, and Z. M. Abbood, Impact of Soil Temperature and Precipitation on Vegetation Cover Over Selected Stations in Iraq, Asian Journal of Water, Environment and Pollution, 2024, 21(1), pp. 25–33.
36. W. G. Nassif, A. A. Hashim, S. A. Muter, and O. T. Al-Taai, Relationship Between Winds with Surface Roughness and Carbon Dioxide Concentrations Over Iraq, Asian Journal of Water, Environment and Pollution, 2024, 21(1), pp. 89–96.
37. R. M. Ibrahim, Z. M. Abbood, O. T. Al-Taai, and M. M. Ahmed, The Influence of Ozone Depletion Potential Weighted Anthropogenic Emissions of Nitrous Oxide, Asian Journal of Water, Environment and Pollution, 2024, 21(2), pp. 65–73.
38. W. G. Nassif, F. H. S. Lagenean, and O. T. Al-Taai, Impact of vegetation cover on climate change for different regions in Iraq, Journal of Agrometeorology, 2022, 24(2), pp. 138–145.
39. W. G. Nassif, F. H. Jasim, and O. T. Al-Taai, Analysis of air temperature, relative humidity and evaporation over Iraq using ECMWF reanalysis, Indian Journal of Ecology, 2021, 48(2), pp. 446–452.
40. S. J. Al-Jaf, and O. T. Al-Taai, Impact of carbon dioxide concentrations on atmospheric temperature changes over Iraq and some neighboring countries, Plant Archives, 2019, 19, pp. 1450–1456.
41. Z. M. Abbood, and O. T. Al-Taai, Data analysis for cloud cover and rainfall over Baghdad City, Iraq, Plant Archives, 2020, 20(1), pp. 822–826.
42. Z. M. Abbood, O. T. Al-Taai, and W. G. Nassif, Impact of wind speed and direction on low cloud cover over Baghdad city, Current Applied Science and Technology, 2021, 21(3), pp. 590–600.
43. Abd, N.M., Abbood, Z.M., Mohammed, N.A., Al-Taai, O.T., Nassif, W.G. Impact of Acid Gases on Total Precipitation Over Iraqi Stations. Nature Environment and Pollution Technology, 2025, 24, pp. 439–448.
44. Maan, H., Al-Taai, O.T., Halos, S.H. Estimate the drought in some Iraqi meteorological stations using the de Martonne Aridity index. AIP Conference Proceedings, 2024, 3229(1), 050014.

45. Nassif, W.G., Hashim, A.A., Muter, S.A., Al-Taai, O.T. Relationship Between Winds with Surface Roughness and Carbon Dioxide Concentrations Over Iraq. Asian Journal of Water, Environment and Pollution, 2024, 21(1), pp. 89–96.
46. Maan, H., Al-Taai, O.T., Halos, S.H. Calculating the Environmental Drought Index using the de Martonne Equation for the Rainy Months in Iraq. IOP Conference Series: Earth and Environmental Science, 2024, 1371(2), 022001.
47. Hashim, S.A., Tawfeek, Y.Q., Al-Taai, O.T., Abbood, Z.M. Spatiotemporal Distribution of the Monthly and Seasonal Mean of High Vegetation Cover, Total Precipitation, and Temperature in Iraq for the Period (1950-2022). IOP Conference Series: Earth and Environmental Science, 2024, 1371(2), 022008.
48. Ibrahim, R.M., Abbood, Z.M., Al-Taai, O.T., Ahmed, M.M. The Influence of Ozone Depletion Potential Weighted Anthropogenic Emissions of Nitrous Oxide. Asian Journal of Water, Environment and Pollution, 2024, 21(2), pp. 65–73.
49. Al-Amery, H.A., Al-Taai, O.T. The ozone effect on shortwave solar radiation in the atmosphere over Iraq. AIP Conference Proceedings, 2020, 2290, 0027825.
50. Nassif, W.G., Al-Taai, O.T., Muter, S.A. Inference of dynamically dust storms by relying on aerosolos optical thickness in Iraq. Journal of Green Engineering, 2021, 11(1), pp. 530–546.
51. Salman, A.D., Al-Taai, O.T. Association Between Precipitable Water Vapor and Evaporation Over Iraq During the Period (1979-2019). IOP Conference Series: Earth and Environmental Science, 2022, 1060(1), 012021.
52. Al-Awadi, R.S., Al-Taai, O.T., Abdullah, S.A. Assessment of X-Ray Effects on HF Radio Communications. IOP Conference Series: Earth and Environmental Science, 2023, 1223(1), 012003.
53. Al-Behadili, A.A., Al-Taai, O.T., Al-Muhyi, A.H.A. Analysis of ship accident resulting from bad weather conditions in the port of Khor Al-Zubair, Iraqi crane accident Aba Thar: a case study. Bionatura, 2023, 8(1), 49.
54. Al-Taai, O.T. Preface. IOP Conference Series: Earth and Environmental Science, 2023, 1223(1), 011001.
55. Hassan, A.S., Zaki, K.N.. Decadal analysis of carbon dioxide emissions from different state of fossil fuels in Iraq. Indian Journal of Public Health Research and Development, 2018, 9(12), pp. 865–868.